frontiers in Materials

ORIGINAL RESEARCH
published: 25 January 2019
doi: 10.3389/fmats.2019.00003

High-Performance Non-enzymatic Glucose Sensors Based on CoNiCu Alloy Nanotubes Arrays Prepared by Electrodeposition

Xuewen Gong[1,2], Yan Gu[1], Faqiang Zhang[1], Zhifu Liu[1]*, Yongxiang Li[1,3], Guanyu Chen[1,2] and Bo Wang[1]*

[1] CAS Key Laboratory of Inorganic Functional Materials and Devices, Shanghai Institute of Ceramics, Chinese Academy of Sciences, Shanghai, China, [2] Center of Materials Science and Optoelectronics Engineering, University of Chinese Academy of Sciences, Beijing, China, [3] School of Engineering, RMIT University, Melbourne, VIC, Australia

Transition metal alloys are good candidate electrodes for non-enzymatic glucose sensors due to their low cost and high performance. In this work, we reported the controllable electrodeposition of CoNiCu alloy nanotubes electrodes using anodic aluminum oxide (AAO) as template. Uniform CoNiCu alloy arrays of nanotubes about 2 μm in length and 280 nm in diameter were obtained by optimizing the electrodeposition parameters. Scanning electron microscopy (SEM) and energy dispersive X-ray spectroscopy (EDS) measurements indicated that the as-prepared alloy nanotubes arrays are composed of 64.7 wt% Co-19.4 wt% Ni-15.9 wt% Cu. Non-enzymatic glucose sensing measurements indicated that the CoNiCu nanotubes arrays possessed a low detection limit of 0.5 μM, a high sensitivity of 791 μA mM^{-1} cm^{-2} from 50 to 1,551 μM and 322 μA mM^{-1} cm^{-2} from 1,551 to 4,050 μM. Besides, they showed high reliability with the capacity of anti-jamming. Tafel plots showed that alloying brought higher exchange current density and faster reaction speed. The high performance should be due to the synergistic effect of Co, Ni, and Cu metal elements and high surface area of nanotubes arrays.

Keywords: CoNiCu alloy, nanotubes arrays, electrodeposition, non-enzymatic glucose sensors, synergistic effect

OPEN ACCESS

Edited by:
Xiaogan Li,
Dalian University of Technology (DUT), China

Reviewed by:
Yanbai Shen,
Northeastern University, China
Yangong Zheng,
Ningbo University, China

***Correspondence:**
Yan Gu
guyan@mail.sic.ac.cn
Zhifu Liu
liuzf@mail.sic.ac.cn

Specialty section:
This article was submitted to Functional Ceramics, a section of the journal Frontiers in Materials

Received: *03 December 2018*
Accepted: *09 January 2019*
Published: *25 January 2019*

Citation:
Gong X, Gu Y, Zhang F, Liu Z, Li Y, Chen G and Wang B (2019) High-Performance Non-enzymatic Glucose Sensors Based on CoNiCu Alloy Nanotubes Arrays Prepared by Electrodeposition. Front. Mater. 6:3. doi: 10.3389/fmats.2019.00003

INTRODUCTION

With the increasing demand in medical, food, and pharmaceutical industry, more attention has been paid to develop glucose sensors with high sensitivity, high stability, and low price (Yoo and Lee, 2010; Tian et al., 2014; Galant et al., 2015). Although traditional enzymatic glucose sensors have undergone three generations of development and possess high sensitivity and selectivity, they always suffer from the performance variation with environment and the degradation of enzyme activity (Katakis and Dominguez, 1995; Toghill and Compton, 2010). In recent years, non-enzymatic electrochemical glucose sensors based on the oxidation of glucose to gluconolactone on electrode surface arise as a promising candidate for glucose concentrations detection (Lu et al., 2009; Wang et al., 2012). Many non-enzymatic electrode materials have been developed including noble metal nanomaterials (Jena and Raj, 2006) and their alloy (Sun et al., 2015; Wang et al., 2018), transition metals and their alloys (Jafarian et al., 2008; Mu et al., 2011; Liu et al., 2017). Although noble metals exhibit fascinating properties, there are two main drawbacks: (i) The overall kinetics of glucose electrooxidation is too slow to produce a significant Faraday current;

(ii) The activity of the noble electrode is strongly damaged by chloride ions and intermediates adsorbed on electrode surfaces (Tee et al., 2017). Also, noble metals are too expensive for mass production. The oxidation of glucose by transition metal electrode involves the electrontransfer mediation of the multivalentmetal redox couple which leads to better current response and has no fouling by adsorbed interference species. Hence, transition metal electrodes attract much attention for fabrication more active and cheaper non-enzymatic glucose sensors in recent years.

At present, more and more alloy research in glucose detection has replaced pure metal to improve the stability by forming bimetallic structure (Mahshid et al., 2013; Miao et al., 2013; Sheng et al., 2014; Vilana et al., 2015). Wang et al. (2008) synthesized three-dimensional PtPb alloy networks on Ti substrates to overcome the shortcomings of pure metal and significantly improved the performance. Gao et al. (2011) reported a PtNi alloy nanoparticle-Graphene electrode which had a high nanoparticle loading and effective reduction of graphene oxide. Li et al. (2015) studied a series of MCo (M = Cu, Fe, Ni, and Mn) alloy nanoparticles doped carbon nanofibers electrodes and explored the distinction of different alloy sensors. These alloys had higher electrocatalytic activities and stabilities compared with those of pure metals due to the synergistic effect (Luo and Kuwana, 1994; Li et al., 2015; Vilana et al., 2015). Transition metal-based alloy is a prospective direction and worthy of further study for low-cost and high-performance non-enzymatic glucose sensors. In different alloy systems, more attention was paid to cobalt material due to its excellent catalytic ability and chemical stability (Ding et al., 2010; Kung et al., 2011; Madhu et al., 2015; Shu et al., 2018). Unlike the transition metals such as nickel and copper, cobalt could form various oxidation states in alkaline conditions(Hwang et al., 2018).

On the other hand, since the non-enzymatic glucose sensing is based on the electrode surface, the morphology of electrode material will have a large effect on the performance of sensors. Therefore, nanoparticles, nanosheets, nanowires, and other nanomaterials were widely used in glucose sensors research to solve the problem of electrode surface saturated (Liu et al., 2014; Jiang et al., 2017; Zhang et al., 2017). However, some nanomaterials like particles need to be loaded onto other materials which cause interference current and complex production process (Jena and Raj, 2006). Attributed to large surface-to-volume ratio and ordered arrangement, more interest was focused on one-dimensional nanowires and nanotubes structures which was considered as the beneficial dimensionality for electrontransfer (Hu et al., 1999). In order to compare the difference in glucose detection, Li et al. (2014) used Pt-Pd as the electrodes material and demonstrated that nanotubes had a higher activity for glucose electro-oxidation. To the best of our knowledge, no studies concerning ternary transition alloy nanotubes have been reported for glucose sensor yet.

In this work, we fabricated well-aligned cobalt-based ternary alloy nanotubes by using the template-assisted potentiostatic electrodeposition method. The non-enzymatic glucose sensing performance of the alloy nanotubes was investigated. The cobalt-based ternary alloy nanotubes showed excellent performance with low detection limit, wide detection range, and high sensitivity.

EXPERIMENTAL SECTION

The anodic aluminum oxide (AAO) template with diameter of 280 nm was obtained from Top Membranes Technology Ltd. The source materials nickel sulfate hexahydrate, cobalt sulfate, copper sulfate pentahydrate, boric acid, sodium chloride, L-tyrosine, ascorbic acid, and dopamine hydrochloride were purchased from Shanghai Aladdin Biochemical Polytron Technologies Inc. Sodium citrate and ethanol were purchased from China National Pharmaceutical Group Corporation. All chemicals involved were of analytical grade and were used directly. Before the electrodeposition, a thin conductive layer of Au was sputtered onto one side of the AAO template as a working electrode in a three-electrode cell. A platinum sheet was used as the counter electrode and a saturated calomel electrode as the reference electrode. The deposition was carried out at room temperature with different DC voltages and time on a CHI 660C electrochemical working station (Shanghai Chenhua, China). For the ternary alloy deposition, water solution with 0.1 M $CoSO_4{\cdot}7H_2O$, 0.2 M $NiSO_4{\cdot}6H_2O$, 0.01 M $CuSO_4{\cdot}5H_2O$, 0.4 M H_3BO_3, and 0.5 M $Na_3C_6H_5O_7{\cdot}2H_2O$ were used as electrolyte. For comparison, the Co nanotubes arrays were deposited at −1.5 V voltage for 5 min using 0.1 M $CoSO_4{\cdot}7H_2O$, 0.4 M H_3BO_3 water solution as electrolyte. After deposition, the AAO template containing the nanotubes was immersed in a 1 M NaOH solution to remove the template.

The phase composition of the prepared nanotubes was determined by X-ray Diffraction (XRD, D8 DISCOVER DAVINCI). The morphology and microstructure were characterized using field-emission scanning electron microscopy (SEM, SU8220) equipped with an energy dispersive X-ray spectroscopy (EDS). For glucose sensing performance measurement, the nanotubes arrays were transferred to an indium tin oxide (ITO) substrate with a nail polish covered the edge between the ITO and the nanotubes arrays. All of the electrodes were activated by 60 cyclic voltammetry (CV) cycles at a scanning rate of 30 mV s^{-1} in a 0.1 M NaOH solution, respectively, before the performance test. Subsequently, the nanotubes arrays were used for glucose test in the 0.1 M NaOH solution with a different concentration of glucose and 0.4 V was chosen as the working potential for the amperometric performance test. A platinum sheet was used as the counter electrode and an Ag/AgCl electrode as the reference electrode.

RESULTS AND DISCUSSIONS

Fabrication of Nanotubes Arrays

Although template-based electrochemical deposition is a well-accepted process to synthesize nanostructures, the morphology and component of the products could be largely affected by the deposition parameters like applied voltage and deposition time because of the diversity of electrochemical properties of different elements. In this work, we tuned the electrodeposition voltage and time to obtain high-quality alloy nanotubes arrays. The SEM

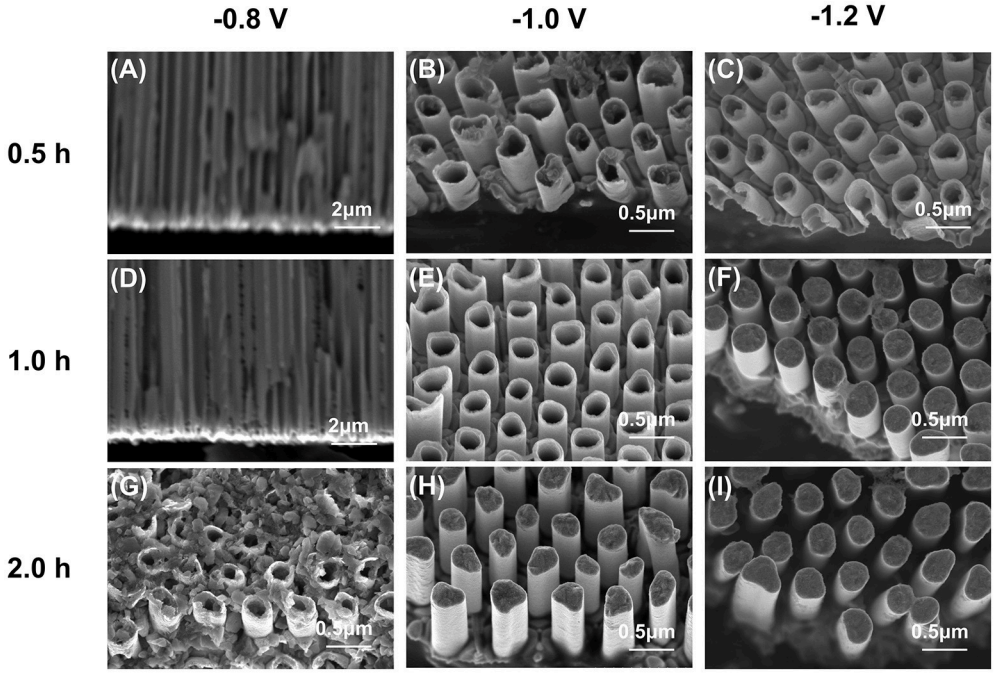

FIGURE 1 | SEM images of the products deposited at different potential and time. **(A,B)** cross-section image with AAO template. **(C–I)** products after removing the AAO template.

images of products synthesized at −0.8, −1.0, and −1.2 V within different deposition time are shown in **Figure 1**. As shown in **Figures 1A,B**, the deposition rate is too slow to observe the product from the cross-section at the low deposition voltage −0.8 V within 1 h. Fortunately, extending the deposition time to 2 h, the short nanotubes arrays are obtained (**Figure 1C**). When the deposition voltage was increased to −1.0 V (**Figures 1D–F**), nanotubes are grown easily in a relatively short time. The wall of nanotubes become thicker with time prolonging (**Figures 1D,E**) and eventually, the nanotubes are filled and nanorods arrays are obtained (**Figure 1F**). When the deposition voltage increases to −1.2 V, nanotubes arrays can also be obtained in half hour (**Figure 1G**). But the wall of the nanotubes is even thicker than these deposited at −1.0 V for 1 h. So, extending the deposition time, only nanorods arrays can be obtained at a deposition voltage of −1.2 V (**Figures 1H,I**).

The possible growth process of alloy nanotubes is illustrated in **Figure 2**. **Figure 2A** is the cross-section of the AAO template. After spraying the gold as the working electrode, some gold particles are sprayed on the bottom wall of the AAO (**Figure 2B**). When deposition voltage applied, high charge density would form near the bottom wall of AAO around gold particles. Such a stronger electrochemical activity makes the alloy conducive to growth along the wall of AAO template (**Figure 2C**). As time goes on, the nanotubes become longer while the thickness increases (**Figures 2D,E**), and finally turn into nanorods (**Figure 2F**). Throughout the process, the influence of the electric field and adsorption energy on the growth of alloy exists which cause different growth priorities and results in the product morphology variation from nanotubes to nanorods (Li et al., 2009). At the initial stage of growth, the alloy grows along the wall of the AAO template, which may be because of the increased metal ion concentration around the wall of AAO template induced by surface absorption and the existence of conductive particles in tubes. Considering the narrow channel between electrolyte and cathode surface, the metal ion concentration around the AAO has a dominating effect in the initial electrodeposition process. These reasons make the growth of nanotubes more favorable in the early stage of deposition. But with the extension of time, the wall of nanotubes gets thicker gradually. The adsorption effect becomes weaker and the electric field effect is more prominent. The nanoparticles begin to stack inside the tubes until the product are completely filled. Besides, the increase of voltage is helpful to deposit. But the growth rate is too fast to control when the voltage is too high.

Thus, it is clear that the voltage and time play a critical role during the formation of nanotubes. We choose the deposition voltage of −1.0 V and deposition time for 1 h to do more detailed study after taking into account all the above-mentioned experimental condition. The morphology and composition of the nanotubes are shown in **Figure 3**. The high magnification of SEM observation (**Figure 3A**) reveals that well-aligned CoNiCu nanotubes are formed on the substrate face. The diameter of nanotubes is about 280 nm, indicating that the nanotubes grow along the wall. The average length of the nanotubes is about 2 μm from the cross-section image (**Figure 3B**). The result of EDS shown in **Figure 3C** confirms that the nanotubes are composed of 64.7 wt% Co-19.4 wt% Ni-15.9 wt% Cu. The Al, O, and Au peaks

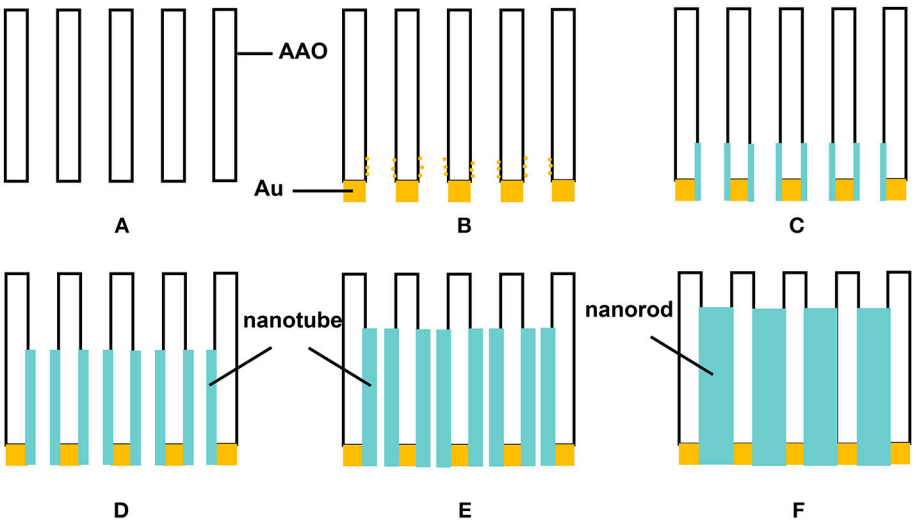

FIGURE 2 | Schematic diagram of the growth of alloy nanotubes. **(A)** section of AAO template, **(B)** section after spraying gold, **(C–F)** deposition process in template.

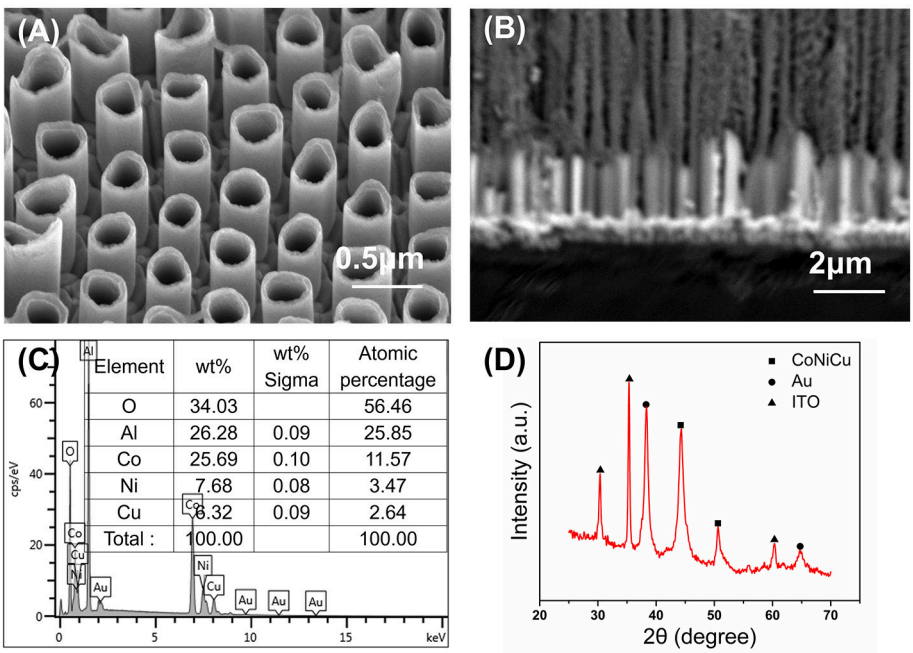

FIGURE 3 | CoNiCu nanotubes arrays with applied potential −1.0 V **(A)** dissolving the AAO template; **(B)** cross-section image embedded in AAO channels; **(C)** energy dispersive spectra of CoNiCu embedded in AAO channels; **(D)** XRD patterns of prepared nanotubes arrays transferred on ITO.

originate from the AAO temple. The crystal phase of CoNiCu nanotubes was further confirmed by XRD. The XRD patterns (**Figure 3D**) indicate that the nanotubes are of high crystallinity. The background interfering peaks are due to residual alumina, ITO, and Au. Furthermore, no peaks assigned to the pure metals are observed which reveals a ternary alloy was formed.

It is worth noting that the difference in deposition potential will be a problem to handle the composition. The standard electrode potentials for Co, Ni, Cu deposition are −0.277, −0.257, and 0.159 V, respectively. The more positive the potential is, the easier the metal ions are to reduce. It is clear that the reduction of copper is most likely to occur. If not controlled, copper will grow more rapid and desired cobalt-based alloy cannot form. And what's worse is, anomalous phenomena occur when it is a co-precipitation of a mixed metal ions system and the growth rate of cobalt is much faster than nickel at low current

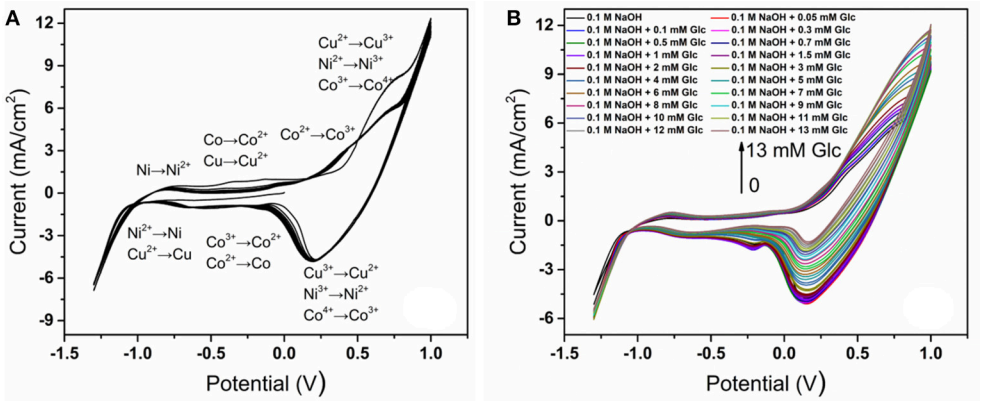

FIGURE 4 | (A) Activated CoNiCu electrode in 0.1 M NaOH by CV for multiple cycles; **(B)** CVs of activated CoNiCu electrode in 0.1 M NaOH + different glucose concentrations.

density typically (Fan and Piron, 1996). So we set the mole concentration of the solution to Co: Ni: Cu = 10: 20: 1. Besides, sodium citrate, as the complex metal ion, is used to guarantee the similar precipitation potential of Co^{2+}, Ni^{2+}, and Cu^{2+} to get controllable components. As a result, uniform CoNiCu alloy nanotubes arrays were obtained at a deposition voltage of −1.0 V for 1 h and were used as electrodes for glucose sensing characterization.

Glucose Sensing Performance Characterization

Cyclic voltammetry is used to activate the electrode and test the reaction response between the electrode and glucose solution. After carried the cyclic voltammetry reaction at a scanning rate of 30 mV s^{-1} in a 0.1 M NaOH solution, the alloy electrode surface is activated. The reaction corresponding to the peak value of cyclic voltammetric curve is deduced in **Figure 4A**. During oxidation, metals are first oxidized to divalent and oxidized to trivalent follow. Ni^{3+} and Cu^{3+} show good chemical stability but Co^{3+} is further oxidized into CoO_2 at higher potential (Liang et al., 2006; Hu et al., 2009).

The possible electrochemical reaction is as follows (Wang et al., 2013; Zhang et al., 2017):

$$Co + 2OH^- \rightarrow Co(OH)_2 + 2e^-$$
$$Co(OH)_2 + OH^- \rightarrow CoOOH + H_2O + e^-$$
$$CoOOH + OH^- \rightarrow CoO_2 + H_2O + e^-$$
$$Ni + 2OH^- \rightarrow Ni(OH)_2 + 2e^-$$
$$Ni(OH)_2 + OH^- \rightarrow NiOOH + H_2O + e^-$$
$$Cu + 2OH^- \rightarrow CuO + H_2O + 2e^-$$
$$CuO + H_2O \rightarrow Cu(OH)_2$$
$$Cu(OH)_2 + OH^- \rightarrow CuOOH + H_2O + e^-$$

A comparative study of electrochemical response on the CoNiCu electrocatalytic performance of different glucose concentrations was conducted in 0.1 M NaOH solution from −1.3 to +1.0 V (**Figure 4B**). With the increase of glucose concentration, the peak current of the alloy electrode varied strongly accompanied by the increase of oxidation current and the decrease of reduction current, demonstrating that the electrode could achieve efficient electrooxidation of glucose. Comparing with the cyclic voltammetric curve of the CoNiCu alloy electrode, the changed electrocatalytic current of alloy electrode indicates that the following reactions occurred:

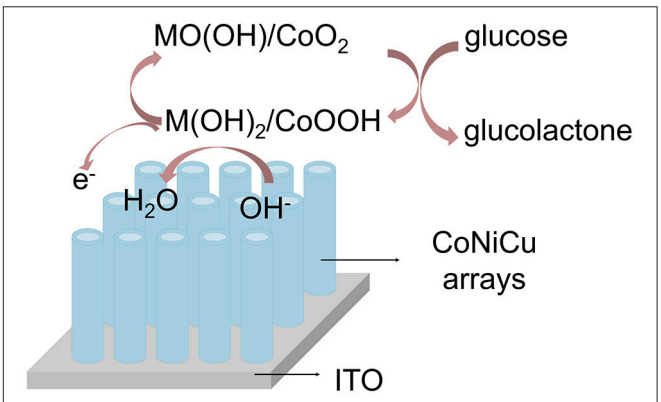

FIGURE 5 | Schematic representation of the glucose electrocatalytic reaction on CoNiCu nanotubes array.

$$2CoO_2 + \text{glucose} \rightarrow 2CoOOH + \text{gluconolactone}$$
$$NiOOH + \text{glucose} \rightarrow Ni(OH)_2 + \text{gluconolactone}$$
$$CuOOH + \text{glucose} \rightarrow Cu(OH)_2 + \text{gluconolactone}$$

Figure 5 shows the schematic illustration of glucose reaction on the CoNiCu nanotubes array under electrochemical condition. According to the "Incipient Hydrous Oxide Adatom Mediator" model Burke proposed (Burke, 1994; Rahman et al., 2010), the metal could be oxidized to $M^{II}(OH)_2$ and following $M^{III}OOH$ or $M^{IV}O_2$ in an alkaline solution. When glucose is added, it is oxidized to gluconolactone by $M^{III}OOH$ or $M^{IV}O_2$. As a result, CV oxidation peak current increases and reduction current

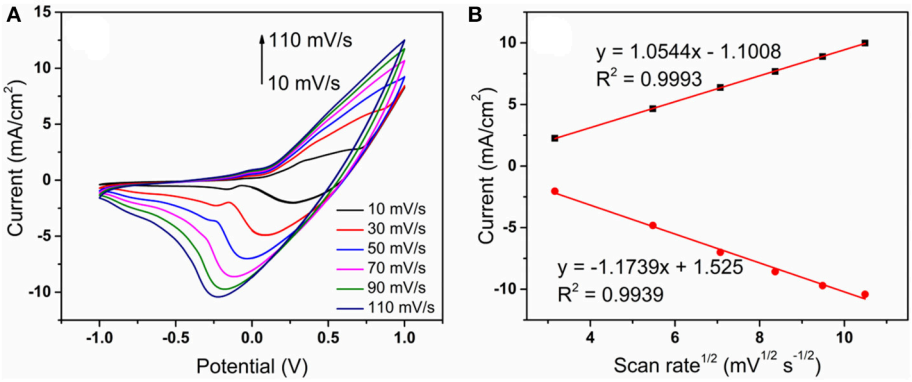

FIGURE 6 | (A) CVs of the CoNiCu electrodes in 0.1 M NaOH + 0.3 mM glucose at different scanning rates (10–110 mV s^{-1}); **(B)** redox peak currents as a function of the square root of the scan rate.

decreases. Different response currents result from different metal elements electrodes and solution environment. The high surface-to-volume ratio and good electron transfer channel of the nanotubes array largely enhanced the electrocatalytic reaction. So, the CoNiCu alloy nanotubes array could be an excellent glucose sensor electrode.

Kinetic study of reaction process is based on the effect of the potential scanning rate in a 0.1 M NaOH solution containing 0.3 mM glucose (**Figure 6**). The result shown in **Figure 6A** displays that the reduction potential shifts negatively and the oxidation potential shifts positively with the increase of scanning speed. Besides, both the anodic and cathodic peak current increase with the scanning rate from 10 to 110 mV s^{-1}. There are good relationships between the peak currents and the square root of the scanning rate (**Figure 6B**). This indicates that it is a diffusion-controlled process on the electrode. The rate of the whole reaction depends on the diffusion process of the ions from the solution to the surface of the electrode. To further investigate the difference after alloying, Co nanotubes electrode was prepared for a comparison. The oxidation peak of Co electrode is at about 0.3 V which is similar to CoNiCu electrode. However, according to existing reports, the anodic peak of the anodic peak of Ni electrode is at about 0.45 V, while that of Cu at about 0.4 V (Lu et al., 2009; Luo et al., 2012). Alloying did not increase the peak position of oxidation. Besides, since Co reacts more preferentially at 0.3 V, electrons could transfer from Ni/Cu to supplement and promote the oxidation of glucose.

To further understand the enhanced performance of CoNiCu nanotubes array, the Tafel plots of the Co nanotubes array, and CoNiCu nanotubes array were obtained in a 0.1 M NaOH with 0.3 M glucose (**Figure 7**). We draw tangents of the two curves at open circuit potential +60∼120 mV to get the Tafel slope and exchange current density (i_0). The Tafel slope of the CoNiCu nanotubes array is close to that of Co nanotubes array, which means they have similar overpotential and reaction activity. But a higher exchange current density i_0 indicates a faster reaction speed of CoNiCu nanotubes array electrode. This might be because the alloying expands the lattice which causes the d-band state changing and increases the adsorption of the

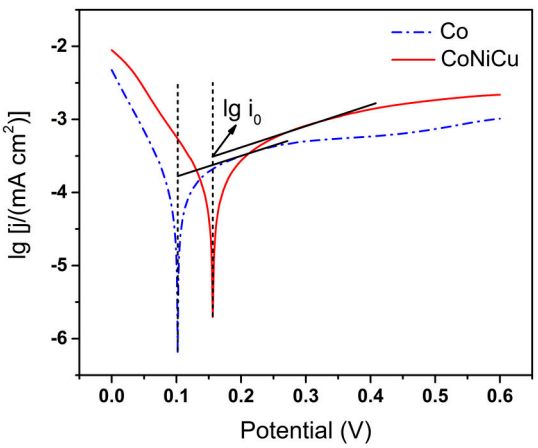

FIGURE 7 | Tafel plots of Co and CoNiCu electrodes in 0.1 M NaOH + 0.3 mM glucose.

reactants. As a result, the reaction is promoted (Groß, 2006). This kind of synergistic effect of three different metals should large contribution to the excellent performance of the ternary alloy nanotubes.

In order to quantitatively analyze the variation of sensor response current with the concentration glucose, the current is measured by continuously dropping glucose solution under a constant voltage. As can be seen from **Figure 6A**, there is a current peak near 0.3–0.6 V at the low scan rate. So we choose the potential of 0.4 V to do the amperometric test. **Figure 8** shows the amperometric response of CoNiCu electrode with a successive addition of glucose to a 0.1 M NaOH solution. A low stirring rate (150 rpm) was used to accelerate mixing during the experiment. Inset of **Figure 8A** is the glucose response current curve at extremely low concentration. Although the noise current is very large, we could see an obvious trend of current rising at about 0.5 μM. In order to get a more accurate linear curve of current varying with glucose concentration, the linear experiment was started from 50 μM. As shown in **Figure 8A**, once injected the

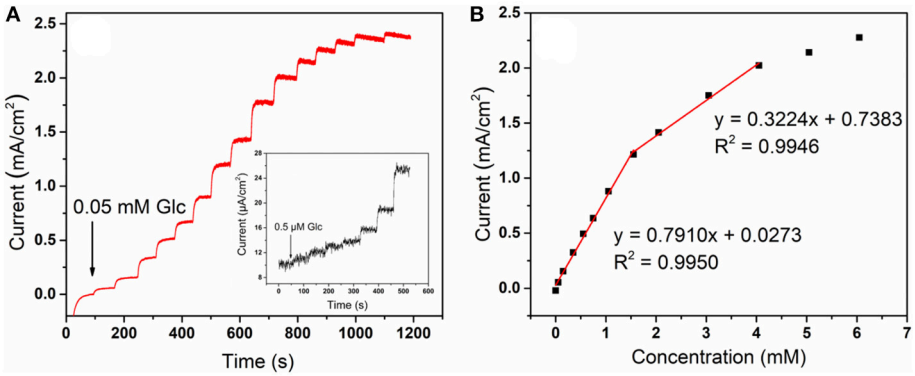

FIGURE 8 | (A) Amperometric response of CoNiCu electrode with a successive addition of glucose from 0.05 to 6 mM at 0.4 V. Inset: a successive addition of glucose from 0.5 to 11 μM; **(B)** the linear correlation between the concentration and response current of CoNiCu electrode.

TABLE 1 | Comparison of Co-based ternary alloy non-enzymatic glucose sensors.

Electrode materials	Sensitivity ($\mu A\ mM^{-1}\ cm^{-2}$)	Linear range (μM)	LOD (μM)	Operation potential (V)	Medium	References
CuCo-carbon nanofibers	507	20–1100	1.0	+0.6	0.1 M NaOH	Li et al., 2015
NiCu/GC	–	1000–9000	0.8	+0.54 vs. Ag/AgCl	1 M NaOH	Jafarian et al., 2008
$Co_{0.7}Ni_{0.3}$ nanorods	544	100–1000	–	0.5–0.65	0.1 M NaOH	Vilana et al., 2015
$Co_{0.6}Ni_{0.4}$ nanorods	383	100–1000	–	0.5–0.65	0.1 M NaOH	
CoNiCu nanotubes arrays	791	50–1551	0.5	+0.4 vs. Ag/AgCl	0.1 M NaOH	our work
	322	1551–4050				

glucose to the solution, the current responded immediately and it was stable in <5 s. We also noticed that the noise current increases with the increase of concentration, which may have an impact on the current acquisition. But, throughout the testing process, the signal-to-noise(S/N) ratio of the collected current is still more than three times. By collecting the current in each stable state, relation of the current intensity on the different glucose concentrations is displayed in **Figure 8B**. The electrode has a low detection limit (0.5 μM) and two-segment linear regions with a high sensitivity of 791 $\mu A\ mM^{-1}\ cm^{-2}$ from 50 to 1,551 μM and 322 $\mu A\ mM^{-1}\ cm^{-2}$ from 1,551 to 4,050 μM. Such a good performance may be attributed to the large surface area of the well-aligned nanotubes structure which provides more sites for the redox reaction. Transition metals with excellent electrical conductivity could also offer good charge transmission channels. The performance of CoNiCu nanotubes array was compared with other Co-based alloys glucose sensors reported previously. As listed in **Table 1**, CoNiCu nanotubes arrays exhibit ultrahigh sensitivity, low limit of detection (LOD), and wide linear range. In addition, the operating potential of CoNiCu nanotubes arrays is lower than others. Low voltage will reduce the response current, but it is more energy efficient in actual use and avoids the influence of possible intermediates which is also a development trend for non-enzymatic glucose sensors (Sun et al., 2015).

Biosensors are eventually used in complex organisms which contain complicated electroactive species such as ascorbic acid (AA), dopamine (DA), L-tyrosine, and sodium chloride

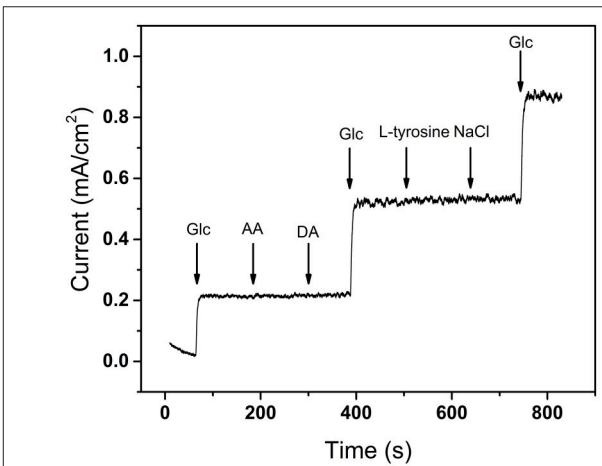

FIGURE 9 | Amperometric response of CoNiCu electrode to a successive addition of glucose and interferences.

(NaCl). Normally, a transition metal-based electrode could also oxidize part of small organic molecules after the formation of $M^{III}OOH$, making the interferential response hard to be avoided (Fleischmann et al., 1972). The selectivity is one of the important criteria for judging whether a sensor is qualified. According to the normal physiological level, the selectivity

of CoNiCu nanotubes array electrode was investigated by a successive addition of glucose, 0.017 mM AA, 0.017 mM DA, 0.017 mM L-tyrosine, and 0.05 mM NaCl, separately. As shown in **Figure 9**, the negligible interferential signal occurs which prove that the CoNiCu nanotubes array has good glucose selectivity. The high sensitivity, LOD, wide linear range, high selectivity, and the relative low price of the CoNiCu alloy nanotubes arrays indicate that it could be a promising electrode material for high performance non-enzymatic glucose sensors.

CONCLUSION

Uniform CoNiCu alloy nanotubes arrays were prepared using a template-assisted electrodeposition method. Deposition voltage and time are the key factors to control the morphology of the ternary alloy. The glucose sensing properties of CoNiCu alloy nanotubes arrays were systematically investigated. The non-enzymatic glucose sensors based on CoNiCu electrodes exhibit higher sensitivity, wider linear range, low operation potential, and high selectivity to glucose compared to those of reported single or binary alloy electrodes. Co is the active element of the CoNiCu alloy nanotubes array. The synergistic effect of the three metals leads to the high performance, which makes the CoNiCu alloy nanotubes array a promising electrode for non-enzymatic glucose sensors.

AUTHOR CONTRIBUTIONS

GX, GY, and LZ contributed conception and design of the study. GX is responsible for experiments and performed the statistical analysis with the help of ZF, CG, and WB. GX and LZ wrote the manuscript. All authors listed have made a substantial, direct and intellectual contribution to the work, and approved it for publication.

ACKNOWLEDGMENTS

We acknowledge the financial support from the National Natural Science Foundation of China (61601444, 61501438) and Youth Innovation Promotion Association of CAS.

REFERENCES

Burke, L. D. (1994). Premonolayer oxidation and its role in electrocatalysis. *Electrochim. Acta* 39, 1841–1848. doi: 10.1016/0013-4686(94)85173-5

Ding, Y., Wang, Y., Su, L., Bellagamba, M., Zhang, H., and Lei, Y. (2010). Electrospun Co3O4 nanofibers for sensitive and selective glucose detection. *Biosens. Bioelectron*. 26, 542–548. doi: 10.1016/j.bios.2010.07.050

Fan, C., and Piron, D. L. (1996). Study of anomalous nickel-cobalt electrodeposition with different electrolytes and current densities. *Electrochim. Acta* 41, 1713–1719. doi: 10.1016/0013-4686(95)00488-2

Fleischmann, M., Korinek, K., and Pletcher, D. (1972). The oxidation of hydrazine at a nickel anode in alkaline solution. *J Electroanal. Chem. Interfacial Electrochem*. 31, 39–49. doi: 10.1016/S0022-0728(72)80425-X

Galant, A. L., Kaufman, R. C., and Wilson, J. D. (2015). Glucose: detection and analysis. *Food Chem*. 188, 149–160. doi: 10.1016/j.foodchem.2015.04.071

Gao, H., Xiao, F., Ching, C. B., and Duan, H. (2011). One-step electrochemical synthesis of PtNi nanoparticle-graphene nanocomposites for nonenzymatic amperometric glucose detection. *ACS Appl. Mater. Interfaces* 3, 3049–3057. doi: 10.1021/am200563f

Groß, A. (2006). Reactivity of bimetallic systems studied from first principles. *Top. Catal*. 37, 29–39. doi: 10.1007/s11244-006-0005-x

Hu, J., Odom, T. W., and Lieber, C. M. (1999). ChemInform abstract: chemistry and physics in one dimension: synthesis and properties of nanowires and nanotubes. *Acc.Chem.Res*. 32, 435–445 doi: 10.1021/ar9700365

Hu, Z.-A., Xie, Y.-L., Wang, Y.-X., Wu, H.-Y., Yang, Y.-Y., and Zhang, Z.-Y. (2009). Synthesis and electrochemical characterization of mesoporous CoxNi1–x layered double hydroxides as electrode materials for supercapacitors. *Electrochim Acta* 54, 2737–2741. doi: 10.1016/j.electacta.2008.11.035

Hwang, D. W., Lee, S., Seo, M., and Chung, T. D. (2018). Recent advances in electrochemical non-enzymatic glucose sensors - a review. *Anal. Chim. Acta* 1033, 1–34. doi: 10.1016/j.aca.2018.05.051

Jafarian, M., Forouzandeh, F., Danaee, I., Gobal, F., and Mahjani, M. G. (2008). Electrocatalytic oxidation of glucose on Ni and NiCu alloy modified glassy carbon electrode. *J Solid State Electrochem*. 13, 1171–1179. doi: 10.1007/s10008-008-0632-1

Jena, B. K., and Raj, C. R. (2006). Enzyme-free amperometric sensing of glucose by using gold nanoparticles. *Chemistry* 12, 2702–2708. doi: 10.1002/chem.200501051

Jiang, J., Zhang, P., Liu, Y., and Luo, H. (2017). A novel non-enzymatic glucose sensor based on a Cu-nanoparticle-modified graphene edge nanoelectrode. *Anal. Methods* 9, 2205–2210. doi: 10.1039/c7ay00084g

Katakis, I., and Dominguez, E. (1995). Characterization and stabilization of enzymebiosensors. *Trac Trends Anal. Chem*. 14, 310–319.

Kung, C. W., Lin, C. Y., Lai, Y. H., Vittal, R., and Ho, K. C. (2011). Cobalt oxide acicular nanorods with high sensitivity for the non-enzymatic detection of glucose. *Biosens. Bioelectron*. 27, 125–131. doi: 10.1016/j.bios.2011.06.033

Li, M., Liu, L., Xiong, Y., Liu, X., Nsabimana, A., Bo, X., et al. (2015). Bimetallic MCo (M=Cu, Fe, Ni, and Mn) nanoparticles doped-carbon nanofibers synthetized by electrospinning for nonenzymatic glucose detection. *Sens. Actuat. B Chem*. 207, 614–622. doi: 10.1016/j.snb.2014.10.092

Li, X., Wang, Y., Song, G., Peng, Z., Yu, Y., She, X., et al. (2009). Synthesis and growth mechanism of Ni nanotubes and nanowires. *Nanoscale Res. Lett*. 4, 1015–1020. doi: 10.1007/s11671-009-9348-0

Li, Y., Niu, X., Tang, J., Lan, M., and Zhao, H. (2014). A Comparative study of nonenzymatic electrochemical glucose sensors based on Pt-Pd nanotube and nanowire arrays. *Electrochim. Acta* 130, 1–8. doi: 10.1016/j.electacta.2014.02.123

Liang, Y.-Y., Bao, S.-J., and Li, H.-L. (2006). Nanocrystalline nickel cobalt hydroxides/ultrastable Y zeolite composite for electrochemical capacitors. *J. Solid State Electrochem*. 11, 571–576. doi: 10.1007/s10008-006-0197-9

Liu, X., Yang, W., Chen, L., and Jia, J. (2017). Three-dimensional copper foam supported CuO nanowire arrays: an efficient non-enzymatic glucose sensor. *Electrochim. Acta* 235, 519–526. doi: 10.1016/j.electacta.2017.03.150

Liu, Y., Zhang, Y., Wang, T., Qin, P., Guo, Q., and Pang, H. (2014). Mesoporous Ni0.3Co2.7O4 hierarchical structures for effective non-enzymatic glucose detection. *RSC Adv*. 4, 33514–33519. doi: 10.1039/c4ra02665a

Lu, L. M., Zhang, L., Qu, F. L., Lu, H. X., Zhang, X. B., Wu, Z. S., et al. (2009). A nano-Ni based ultrasensitive nonenzymatic electrochemical sensor for glucose: enhancing sensitivity through a nanowire array strategy. *Biosens. Bioelectron*. 25, 218–223. doi: 10.1016/j.bios.2009.06.041

Luo, J., Jiang, S., Zhang, H., Jiang, J., and Liu, X. (2012). A novel non-enzymatic glucose sensor based on Cu nanoparticle modified graphene sheets electrode. *Anal. Chim. Acta* 709, 47–53. doi: 10.1016/j.aca.2011.10.025

Luo, P. F., and Kuwana, T. (1994). Nickel-titanium alloy electrode as a sensitive and stable LCEC detector for carbohydrates. *Anal. Chem*. 66, 2775–2782. doi: 10.1021/ac00089a028

Madhu, R., Veeramani, V., Chen, S. M., Manikandan, A., Lo, A. Y., and Chueh, Y. L. (2015). Honeycomb-like porous carbon-cobalt oxide nanocomposite for high-performance enzymeless glucose sensor and supercapacitor applications. *ACS Appl. Mater. Interfaces* 7, 15812–15820. doi: 10.1021/acsami.5b04132

Mahshid, S. S., Mahshid, S., Dolati, A., Ghorbani, M., Yang, L., Luo, S., et al. (2013). Electrodeposition and electrocatalytic properties of Pt/Ni–Co

nanowires for non-enzymatic glucose detection. *J. Alloys Comp*. 554, 169–176. doi: 10.1016/j.jallcom.2012.10.186

Miao, Y., Wu, J., Zhou, S., Yang, Z., and Ouyang, R. (2013). Synergistic effect of bimetallic Ag and Ni alloys on each other's electrocatalysis to glucose oxidation. *J. Electrochem. Soc*. 160, B47–B53. doi: 10.1149/2.059304jes

Mu, Y., Jia, D., He, Y., Miao, Y., and Wu, H. L. (2011). Nano nickel oxide modified non-enzymatic glucose sensors with enhanced sensitivity through an electrochemical process strategy at high potential. *Biosens. Bioelectron*. 26, 2948–2952. doi: 10.1016/j.bios.2010.11.042

Rahman, M. M., Ahammad, A. J., Jin, J. H., Ahn, S. J., and Lee, J. J. (2010). A comprehensive review of glucose biosensors based on nanostructured metal-oxides. *Sensors* 10, 4855–4886. doi: 10.3390/s100504855

Sheng, Q., Mei, H., Wu, H., Zhang, X., and Wang, S. (2014). PtxNi/C nanostructured composites fabricated by chemical reduction and their application in non-enzymatic glucose sensors. *Sens. Actuat. B Chem*. 203, 588–595. doi: 10.1016/j.snb.2014.06.090

Shu, Y., Li, B., Chen, J., Xu, Q., Pang, H., and Hu, X. (2018). Facile synthesis of ultrathin nickel-cobalt phosphate 2D nanosheets with enhanced electrocatalytic activity for glucose oxidation. *ACS Appl. Mater. Interfaces* 10, 2360–2367. doi: 10.1021/acsami.7b17005

Sun, Y., Yang, H., Yu, X., Meng, H., and Xu, X. (2015). A novel non-enzymatic amperometric glucose sensor based on a hollow Pt–Ni alloy nanotube array electrode with enhanced sensitivity. *RSC Adv*. 5, 70387–70394. doi: 10.1039/c5ra13383a

Tee, S. Y., Teng, C. P., and Ye, E. (2017). Metal nanostructures for non-enzymatic glucose sensing. *Mater. Sci. Eng. C Mater. Biol. Appl*. 70, 1018–1030. doi: 10.1016/j.msec.2016.04.009

Tian, K., Prestgard, M., and Tiwari, A. (2014). A review of recent advances in nonenzymatic glucose sensors. *Mater. Sci. Eng. C Mater. Biol. Appl*. 41, 100–118. doi: 10.1016/j.msec.2014.04.013

Toghill, K. E., and Compton, R. G. (2010). Electrochemical non-enzymatic glucose sensors: a perspective and an evaluation. *Int. J. Electrochem. Sci*. 5, 1246–1301. Available online at: http://www.electrochemsci.org/papers/vol5/5091246.pdf

Vilana, J., Lorenzo, M., Gómez, E., and Vallés, E. (2015). Electrochemical deposition of CoNi micro/nanostructures as new materials for electrochemical sensing of glucose. *Mater. Lett*. 159, 154–158. doi: 10.1016/j.matlet.2015.06.116

Wang, G., Lu, X., Zhai, T., Ling, Y., Wang, H., Tong, Y., et al. (2012). Free-standing nickel oxide nanoflake arrays: synthesis and application for highly sensitive non-enzymatic glucose sensors. *Nanoscale* 4, 3123–3127. doi: 10.1039/c2nr30302g

Wang, J., Thomas, D. F., and Chen, A. (2008). Nonenzymatic electrochemical glucose sensor based on nanoporous PtPb networks. *Anal. Chem*. 80, 997–1004. doi: 10.1021/ac701790z

Wang, L., Lu, X., Ye, Y., Sun, L., and Song, Y. (2013). Nickel-cobalt nanostructures coated reduced graphene oxide nanocomposite electrode for nonenzymatic glucose biosensing. *Electrochim. Acta* 114, 484–493. doi: 10.1016/j.electacta.2013.10.125

Wang, L., Zhu, W., Lu, W., Qin, X., and Xu, X. (2018). Surface plasmon aided high sensitive non-enzymatic glucose sensor using Au/NiAu multilayered nanowire arrays. *Biosens. Bioelectron*. 111, 41–46. doi: 10.1016/j.bios.2018.03.067

Yoo, E.-H., and Lee, S.-Y. (2010). Glucose biosensors: an overview of use in clinical practice. *Sensors* 10, 4558–4576. doi: 10.3390/s100504558

Zhang, L., Ye, C., Li, X., Ding, Y., Liang, H., Zhao, G., and Wang, Y. (2017). A CuNi/C nanosheet array based on a metal–organic framework derivate as a supersensitive non-enzymatic glucose sensor. *Nano Micro Lett*. 10:28. doi: 10.1007/s40820-017-0178-9

Conflict of Interest Statement: The authors declare that the research was conducted in the absence of any commercial or financial relationships that could be construed as a potential conflict of interest.